View Article Online / Journal Homepage / Table of Contents for this issue

On-line laser Raman spectroscopic probing of droplets engineered in microfluidic devices

Galder Cristobal,[a] Laurence Arbouet,[a] Flavie Sarrazin,[a] David Talaga,[b] Jean-Luc Bruneel,[b] Mathieu Joanicot[a] and Laurent Servant[b]

Received 22nd February 2006, Accepted 22nd May 2006
First published as an Advance Article on the web 6th June 2006
DOI: 10.1039/b602702d

Sub-nanolitre droplets engineered in microfluidic devices constitute ideal microreactors to investigate the kinetics of chemical reactions on the millisecond time scale. Up to date, fluorescence detection has been extensively used in chemistry and biology to probe reactants and resultant products within such nanodroplets. However, although fluorescence is a very sensitive technique, it lacks intrinsic specificity as frequently fluorescent labels need to be attached to the species of interest. This weakness can be overcome by using vibrational spectroscopy analysis. As an illustrative example, we use confocal Raman microspectroscopy in order to probe the concentration profiles of two interdiffusing solutes within nanolitre droplets transported through a straight microchannel. We establish the feasibility of the experimental method and discuss various aspects related to the space-time resolution and the quantitativeness of the Raman measurements. Finally, we demonstrate that the droplet internal molecular mixing is strongly affected by the droplet internal flow.

Published on 06 June 2006. Downloaded on 25/01/2016 00:28:05.

I. Introduction

Microfluidics and micro total analytical systems (μTAS) are nowadays subject of a huge number of theoretical and experimental studies.[1,2] This interest is motivated in part, by the fundamental questions raised when fluids are subjected to flow in microconfined environments, but also because the emerging microfluidics field offers new paths to face the current needs for high-throughput chemical synthesis and screening. These questions require miniaturization in order to downscale the liquid amounts and an increase of the number and the frequency of experiments. These are key issues for the design of the so called "lab-on-a-chip" systems which look towards the integration into small geometries of all the modules required to heat, sort, disperse, and mix reagents in order to initiate a physical or a chemical transformation and finally to analyse the result.[3,4]

A possible strategy to achieve this is to use nanolitre volume droplets inside which chemical reagents are inserted in a controlled way.[5–7,30] These droplets represent ideal micro-reactors as the reactants are confined in a hundreds of pL volume and because a rapid mixing can easily be achieved. Indeed, Ismagilov *et al.*[5,6] have demonstrated that it is possible to accurately inject steady streams of fluid within droplets and to achieve rapid mixing by making droplets flow in curved channels. Such reactants filled droplets may be issued from the emulsification process of a multiple fluid coflow immersed in an immiscible carrier fluid. Providing the incoming reactant streams are separated by intermediate neutral streams, the reactant fluids only meet and mix once the droplets are formed and not before. This allows the chemical reaction to take place only within the drop. The so-formed multicomponent droplets represent ideal sub-nanolitre microreactors that flow within the channels carried by the continuous phase. As the droplet formation is a one by one process, and all the droplets are formed at the same experimental conditions (low Reynolds numbers, laminar flow) the polydispersity of the sequential droplets is less than 0.5%.[8,9] A special case of interest is when the droplet size is bigger or comparable to the section of the channel. In this case the whole system is described by a "plug-flow", where all the "slugs" move at the same constant speed U all along the channel. Consequently, an explicit correspondence exists between the time t and the droplets travelled distance d within the channel. This can be expressed through the linear relation $d = U\,t$ where U stands for the droplet speed. This steady flow scenario makes this system very well suited for the investigation of the kinetics of chemical or physical processes ranging from the milliseconds to minutes or hours if the channels are sufficiently long. Indeed, by controlling precisely the location y of a spatially resolved analytical probe along the channel, it is possible to analyse the chemical composition of the droplets containing the reactive species at a specific time t of their evolution, $t = y/U$.

The detection and analysis of the chemical compounds carried within the droplets remains thus a major issue of significance. The ideal analytical probe should combine specificity, selectivity and spatial resolution. The probing of the local compositions of the circulating droplets has been already reported by using fluorescence and UV-visible absorption spectroscopy. However, such approaches rely on the presence of chromophores in the injected fluids and although they are very sensitive, they lack specificity. On the other hand, although vibrational spectroscopy might be less sensitive than the previous two techniques, it is intrinsically more selective.

[a]*Rhodia-CNRS Laboratory of the Future 178 avenue du Docteur Schweitzer, 33600, Pessac, France*
[b]*Laboratoire de Physico-Chimie Moléculaire, UMR 5803 351, cours de la Libération, 33405, Talence Cedex, France*

 This journal is © The Royal Society of Chemistry 2006

View Article Online

Published on 06 June 2006. Downloaded on 25/01/2016 00:28:05.

Nevertheless, the poor sensitiveness can be compensated by using long acquisition times thanks to the steady state of the flow or by using enhancement approaches such as resonance Raman scattering.[10,11] Furthermore, the recent coupling of infrared and Raman spectrometers with optical microscopes makes of these spectroscopic techniques well suited tools to probe micro total analysis systems. Lendl *et al.*[12] adapted to a micro-mixing device an infrared spectroscopy setup which was designed to resolve temporally chemical reactions. Lately, Salmon *et al.*[13] have used a Raman microspectroscopy device to investigate the kinetics of chemical reactions and the interdiffusion of non-reacting fluids within microchannels which operate under flow control.[14]

In this report, we demonstrate that it is possible to use Raman confocal microspectroscopy to probe the composition of circulating droplets engineered in microfluidic devices. The paper is organized as follows: we first describe the strategy we chose to produce droplets in microchannels and we review the various parameters that affect their shape, size and production frequency among others. We then describe a first model experiment where we couple a microfluidic plateform with a confocal Raman microscope. We describe how we can use the Raman signal recorded within the channel to investigate the properties of the flowing two phase stream. More specifically, we investigate how we can get insights in the droplet size and production frequency by analyzing the various parts of the spectra. Finally, we address spatial resolution issues by investigating the mixing of two model aqueous solutions confined initially in each hemisphere of a droplet. These results show that Raman microscopy is ideally suited to probe fluid mixing in such droplets, and more generally, to analyse chemical composition of fluids hosted by such droplets.

II. Experimental

The microfluidic devices were fabricated with poly(dimethylsiloxane) (PDMS) by using rapid prototyping[15–17] and conventional soft lithography techniques.[18] A transparency mask of 20 000 dpi resolution (CAD/Art Services Inc., California) was used in 1 : 1 contact photolithography with SU-8 phororesist (MicroChem, Newton, MA) to generate a negative "master" consisting of patterned SU-8 photoresist on a silicon flat surface. Positive replicas were performed by molding a mixture 10 : 1 of PDMS with a temperature active cross-linker against the master. After curing the whole for an hour at 65 °C, the PDMS was peeled off the silicon surface and holes were performed with a sharp puncher. The PDMS surface and a clean glass surface were activated for 20 seconds[19] with a UVO-cleaner (Jelight 144AX) and both surfaces were immediately brought together. An irreversible seal was formed between the PDMS surface and the glass substrate.

Among the various possible strategies to engineer aqueous droplets in oil within microchannels,[20–23] we used the so called "flow focusing" geometry.[8,24,25] In such geometry, Anna *et al.* have reported the existence of a wide range of drop patterns when water and oil flow rates are varied.[8] The droplet formation phase diagram is complex and while both monodisperse and polydisperse size distributions are observed, the mean droplet size does not seem to depend on the water to oil flow rate ratios. Nevertheless, the benefit of using the "flow focusing" geometry compared to other channel geometries[5,6,20,21] is to dispose of a broader range of droplet sizes in the monodisperse regime. In a "flow focusing" junction the smallest droplet size is defined by the nozzle size whereas in the alternative "T" junction it is imposed by the channel section. Fig. 1 illustrates the microfluidic pattern of the flow focusing geometry designed for the experiment. In this channel geometry, two oil inlets and an aqueous inlet are forced to flow through a channel restriction located downstream the junction resulting in the formation of aqueous droplets. This geometry slightly differs from the geometry suggested by Anna and co-workers[8] in the way that the large reservoir located downstream the orifice is replaced in our case by a 100 micron width channel. The so formed aqueous droplet flow can be characterized by the droplet length (L_{aq}) and the extension of the oil phase separating two consecutive droplets (L_{oil}), as shown in Fig. 1.

Raman spectra were obtained with a confocal Raman microscope (LabRAM system, Jobin-Yvon/Dilor) consisting of a Raman spectrometer coupled to a microscope (model BX 40, Olympus). A $\times 50$ microscope objective was used for focusing the 514 nm beam wavelength of an argon ion laser (Spectra Physics, model 2017) and for collecting the Raman scattered light. The confocal hole was 100 μm so that the extension of the sampling volume was estimated to be roughly a cylinder of 5 μm diameter and 15 μm height. The dispersive spectrometer was equipped with a grating of 1800 lines mm^{-1}, giving a spectral resolution of 3 cm^{-1}. The detector was a Peltier-cooled detector (Wright). The droplet formation and flow velocity within the channels was imaged and controlled through a high speed camera (Phantom V4.2, Vision Research, Inc.) which was coupled to the confocal Raman microscope. We used a homemade Matlab program to analyze the recorded movies in order to obtain information on the droplets formation process, such as production frequency (N), velocity (U) and size (L_{aq} and L_{oil}).

The microfluidic device was mounted on a xyz motorized stage on the microscope. The inlets in the device were connected *via* polyethylene tubing to 1 mL plastic syringes (Becton Dickinson) located at different syringe pumps (Harvard Apparatus, PHD 2000). The fluid flow rates were accurately imposed to the system in a range of 10 to 500 μL h^{-1}. All the

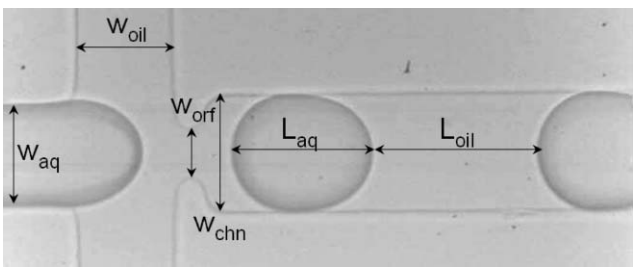

Fig. 1 Droplet formation mechanism in a "flow focusing" junction. The dimensions of the channel geometry are: w_{oil} = 80 μm, w_{aq} = 80 μm, w_{orf} = 30 μm and w_{chn} = 100 μm. In this particular case the water flow rate is 75 μl h^{-1} and the oil flow rate for each the oil inlets is 75 μl h^{-1}. Droplet formation frequency is 75 Hz and droplet velocity is 5 cm s^{-1}.

View Article Online

Published on 06 June 2006. Downloaded on 25/01/2016 00:28:05.

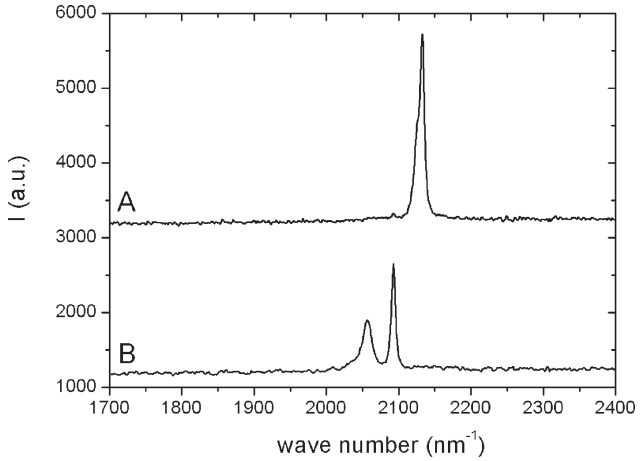

Fig. 2 Raman spectra of droplets containing 0.1 M aqueous solutions of potassium ferrocyanide $K_3Fe(CN)_6$ (A) and potassium ferricyanide $K_4Fe(CN)_6$ (B). Excitation wavelength λ = 514 nm.

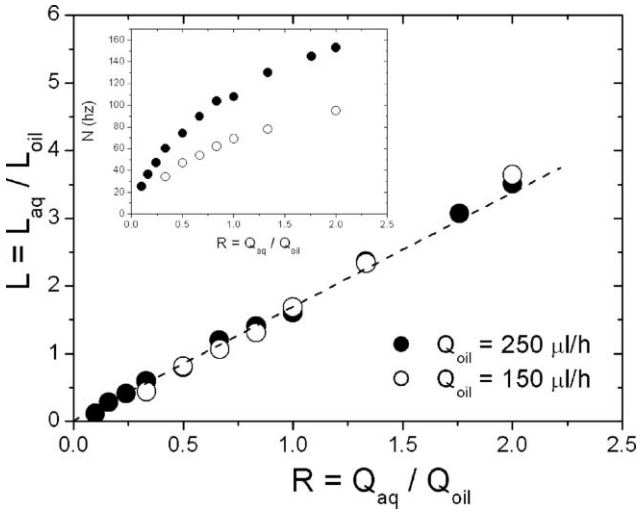

Fig. 3 Lengths ratio (L) variation as a function of the flow rates ratio (R). Inset: droplet break-up frequency (N) variation in function of R.

experiments were performed with a 20cp silicon oil (Rhodisol, Rhodia inc.) as a carrier fluid and two 0.1 M aqueous solutions of $K_4Fe(CN)_6$ and $K_3Fe(CN)_6$ (Sigma Aldrich). The two ferric chemical compounds exhibit sharp Raman lines due to the C=N stretching modes at clearly separated spectral positions, as shown on Fig. 2. Interestingly, the carrier fluid does not exhibit any Raman line in the spectral region (1700–2400 cm^{-1}) of interest.

III. Results

a. Droplet formation: tailoring the size and production frequency

The sizes and production rates of the engineered aqueous droplets depend on both the flow focusing geometry design and on the oil (Q_{oil}) and aqueous (Q_{aq}) flow rates. Previous work have demonstrated that it is essentially the value of the ratio $R = Q_{aq}/Q_{oil}$ which governs the droplet volume whereas the droplet production rate can be tailored by varying concomitantly the fluid flow rates (in order to keep R constant and preserve the droplet size).[24] We qualitatively found the same phase diagram as the one reported by Anna *et al.* except that the monodisperse region in this device was much larger (in Q intervals) than in the precedent geometry.[8] To operate this we worked at two constant oil flow rates: Q_{oil} = 150 µL h^{-1} and 250 µL h^{-1}. We then increased the aqueous flow rates from 15 to 300 µL h^{-1} for Q_{oil} = 150 µL h^{-1} and from 25 to 500 µL h^{-1} for Q_{oil} = 250 µL h^{-1} respectively.

We report on Fig. 3 the influence of the aqueous flow rate (Q_{aq}) on the resultant droplet production for a given value of the continuous phase flow rate (Q_{oil}). The higher the aqueous flow rate (Q_{aq}) the higher the droplet volume (V_{aq}) and the droplet formation frequency (N). This is consistent with the conservation law $Q_{aq} = NV_{aq}$. We show in Fig. 3 that when the flow rate ratio R is increased for a given value of Q_{oil}, the ratio of the system characteristic lengths $L = L_{aq}/L_{oil}$ varies linearly with R. The linear behavior suggests that the droplet volume as well as the continuous phase volume confined between two successive droplets can be written in a simple approximation as $V_i = L_i f_i(w_{chn},h)$, where $f_i(w_{chn},h)$ is a function depending on the height h and the width w_{chn} of the channels. By doing this we describe the flow as a succession of water and oil squished cubic entities with identical widths and L_{aq} and L_{oil} as respective lengths. The slope of the linear dependence between L and R depicted in Fig. 3 contains information about the shape of the droplets.

We have represented on the onset of Fig. 3 the variation of the droplet break-up frequency (N) as a function of R. As R increases, the droplet break-up frequency increases over two decades. It is not the aim of this paper to expand into the details of the mechanisms of droplets formation in "flow-focusing" geometries. This process is complicated and seems to be very geometry dependent.[9,24]

b. Raman sampling conditions

We performed model experiments using a 0.1 M potassium ferricyanide ($K_3Fe(CN)_6$) aqueous solution as the dispersed phase within the droplets. To generate droplets we imposed separately to the continuous and to the aqueous phase a flow rate of Q_{oil} = Q_{aq} = 125 µL h^{-1}. At these flow rates, we measured a droplet break-up frequency of 75 Hz (74.3 Hz) (onset Fig. 3) and the droplet velocity was about 7 cm s^{-1} (6.9 cm s^{-1}). The power of the laser was kept relatively low (10 mwatt) in order to preserve the PDMS integrity, and the acquisition time for a Raman spectrum was 10 seconds, which meant that the Raman signals were averaged over typically 750 droplets. More precisely, the resultant Raman signal recorded during the acquisition time was not only averaged over roughly 750 droplets, but also over the contribution of the silicon oil which was directly probed between two consecutive droplets. It is noteworthy that in the spectral range of interest for the aqueous phase (1700–2400 cm^{-1}), the silicon oil has no specific spectral signatures. However, its contribution to the Raman signal is indirectly detected through the presence of a fluorescence background in the spectrum, which is totally absent from the spectra of pure aqueous samples. The intensity of this fluorescence background is proportional to the amount of silicon oil probed during the acquisition time. The total

 This journal is © The Royal Society of Chemistry 2006

View Article Online

Published on 06 June 2006. Downloaded on 25/01/2016 00:28:05.

collected signal can thus be written as the sum of the signal contributions of the aqueous phase (Raman spectrum I_{aq}) and of the continuous phase (fluorescence background I_{oil}). The total scattered signal is proportional to the analytes concentration, to the measurement time and to the confocal volume:

$$I = I_{aq} + I_{oil}$$

$$I = I_0 \, (K_{aq} \, C_{aq} \, t_{aq} + K_{oil} \, C_{oil} \, t_{oil}) \, V_{confocal}$$

where K_{aq} is a constant incorporating the Raman scattering cross-section of the investigated vibrational mode, whereas K_{oil} is a constant incorporating the fluorescence cross-section of the continuous phase, C_i represents the concentration, t_i is the cumulated acquisition time for each of the phases, $V_{confocal}$ stands for the sampling confocal volume, and I_0 is the incident laser intensity. The above constants (K_i) include additionally various instrumental effects. The respective t_{aq} and t_{oil} times represent the cumulated time during which the aqueous (t_{aq}) and the oil (t_{oil}) phases are probed during a spectral accumulation (t_{total}). It is obvious that the summation of the relative acquisition times is equal to the total acquisition time $t_{aq} + t_{oil} = t_{total} = 10$ s. The relative acquisition times can be expressed as a function of the individual droplet (oil interval) sampling time T_{aq} (T_{oil}) as follows: $t_{aq} = N \, T_{aq} \, t_{total}$ and $t_{oil} = N \, T_{oil} \, t_{total}$. By introducing the characteristic lengths L_{oil} and L_{aq} of each of the phases, we obtain:

$$t_{aq} = N \frac{L_{aq}}{U} t_{total} \text{ and } t_{oil} = N \frac{L_{oil}}{U} t_{total}.$$

In the present picture, the steady state of the droplets flow suggests that the intensity ratio of a characteristic Raman line of the aqueous phase (within the droplets) to that of the fluorescence background of the carrying fluid (oil stream) should scale as the ratio L of L_{aq} to L_{oil}. From the previously developed intensity expressions we have:

$$\frac{I_{aq}}{I_{oil}} = \frac{K_{aq} \, C_{aq} \, N \, T_{aq} \, t_{total} \, V_{confocal}}{K_{oil} \, C_{oil} \, N \, T_{oil} \, t_{total} \, V_{confocal}}$$

which finally reduces to:

$$\frac{I_{aq}}{I_{oil}} = \frac{K_{aq} \, C_{aq} \, L_{aq}}{K_{oil} \, C_{oil} \, L_{oil}} = K \, L$$

This relation emphasizes a linear dependence between the intensity ratio I_{aq}/I_{oil} and L with constant coefficient given by

$$K = \frac{K_{aq} \, C_{aq}}{K_{oil} \, C_{oil}}$$

In order to establish the validity of the above relation, we have carried out experiments where we accurately tailored the droplet size and the droplet production frequency by sequentially increasing the oil and water flow rates. We investigated the Raman response for all the experimental conditions represented in Fig. 3. As we have discussed in the previous paragraph the droplet size (so the length and the curvature) is fixed by the aqueous to oil continuous flow rate ratios (R), and the droplet formation frequency (N) increases by concomitantly increasing the aqueous and oil flow rates (Q_{aq} and Q_{oil}). By controlling the range of R, we have been able for the present experiments to vary the droplet to oil lengths ratio L by a factor of four, and the droplet production frequency over a factor of 10 (10 to 150 Hz). We used the strong Raman vibration band of the ion $Fe(CN)_6^{3-}$ centred at 2050 cm^{-1} to probe the aqueous phase and the fluorescent background of the Raman spectra to evaluate the part of the signal originating from the oil continuous phase. We have displayed on Fig. 4 the ratio of the intensity of the Raman aqueous signal over the intensity of the fluorescence background as a function of $L = L_{aq}/L_{oil}$, for two values of Q_{oil}. As expected in a system where the droplets are constrained by the upper walls of the channels, the intensity ratios clearly exhibit a linear behavior as a function of L.

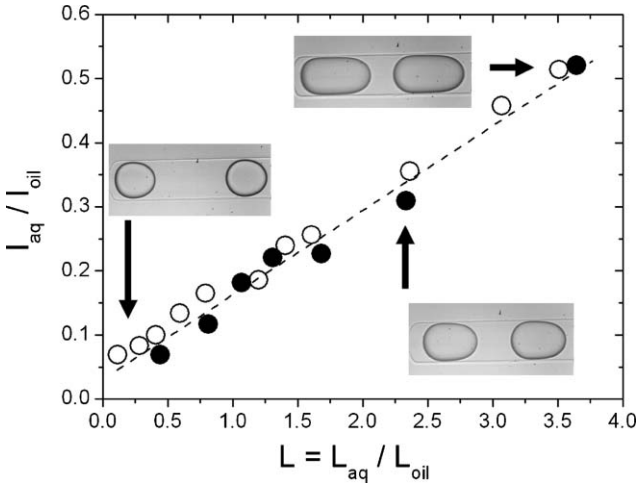

Fig. 4 Aqueous to oil intensities ratio in function of the water to oil lengths ratio. A linear behavior of the intensity ratios is observed for the two sets of parameters: open circles correspond to data taken at Q_{oil} = 150 μL h^{-1} whereas filled circles correspond to Q_{oil} = 250 μL h^{-1}.

It is noteworthy that within the droplet production frequency interval we have investigated (10 to 150 Hz), all the data collapse onto the same linear behavior with respect to L. This result can be understood as a calibration curve, and shows that this approach is quantitative over a large interval of droplet sizes and droplet production frequencies, and offers a way to probe the composition of the droplets. Surprisingly, the line generated by the least-squares method does not cross the origin: this might be ascribed to the fact that for L low values, the flow is not made any more of squashed droplets, but rather by spherical droplets whose diameters are smaller than the channel depth and whose curvature might introduce undesirable reflection and refraction effects for the laser probe.

c. Probing mixing within the droplets

In a second set of experiments, we investigated the mixing of two model solutions within monodisperse droplets under flow. The droplets were engineered in a "flow focusing" junction by emulsifying an unmixed coflow of two miscible aqueous solutions containing 0.1 M aqueous solutions of $K_4Fe(CN)_6$ and $K_3Fe(CN)_6$.[23] The coflow was initiated in a T geometry junction and the miscible fluids flew over a short length path (500 μm) before emulsification. The length of the coflowing channel was designed to be short in order to prevent the interdiffusion of the fluids. The resulting microdroplets present

View Article Online

Published on 06 June 2006. Downloaded on 25/01/2016 00:28:05.

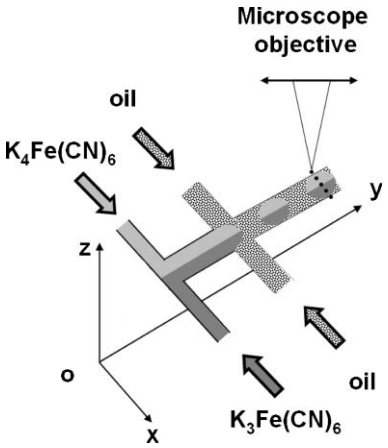

Fig. 5 Two fluids coflow over a short length before they meet two transversal oil streams at the "flow focusing" junction. Droplets presenting two unmixed moieties are dropped off the junction.

a "Janus" structure: a half hemisphere being filled with ferricyanide and the other half filled with ferrocyanide. The interface between the two hemispheres is contained in the y–z plane at the droplet middle position (Fig. 5).

We probed the inner fluid mixing within such droplets by recording Raman spectra along transversal "x-lines" situated at different y positions. Each y position corresponded to a specific time of the evolution of the system through the time–distance equivalence. Along the sampling "x-lines", Raman spectra were recorded every 5 μm which enabled us to take for each y position, 20 spectra in 20 points across the 100 μm width channel. The precise knowledge of the (x,y) coordinates of the laser probe were made possible through the control of the position of the microscope stage. The $K_4Fe(CN)_6$ and $K_3Fe(CN)_6$ flow rates were both adjusted to 75 μL h^{-1} and the silicon oil flow rate was 100 μL h^{-1}. The translation velocity of the droplets was measured to be 25 mm s^{-1} from the images obtained with the high speed camera. We sequentially positioned the microscope objective at various y locations in order to follow the $K_4Fe(CN)_6$ and $K_3Fe(CN)_6$ concentration profiles during mixing for different droplet life-times. The y position was transformed into a temporal variable using the droplet speed U, following the equation $t = y/U$. The acquisition time for each measurement was 10 s, which was equivalent to averaging the signal over 350 droplets. The concentration profiles of the $K_4Fe(CN)_6$ and $K_3Fe(CN)_6$ solutions resulted from the integration of their Raman characteristic lines, as it has been shown in the preceding section.

The collected concentration profiles did reflect the transverse spatial repartition of the chemicals at different droplet lifetimes. However, the so-obtained profiles were highly "affected" by the elliptical shape of the droplets in the y–x plane. In general, at a given x position in the channel, the overall amount of probed matter depends on the longitudinal size of a droplet at this position. When the laser faces the centre of the channel, the droplet probed amount is obviously more important than when it faces a region close to the walls. In order to overcome this artefact introduced by the curved interfaces of the droplets, we divided the concentration profiles by the normalized form factor of a droplet, evaluated from a droplet snapshot by measuring the apparent droplet extension (length) at each transverse x point in the channel. Typically, in the middle of the channel, the probed length is approximately equal to the diameter of the droplet, whereas close to the walls the probed length is close to zero.

The concentration profiles obtained after this operation displayed the spatial distributions of the two chemicals of interest within the droplets and provided a way to probe the mixing state of the system at various droplet lifetimes. As an example, we report on Fig. 6a the concentration profiles obtained at four different y positions corresponding to specific residence times.

The time zero in the above figures corresponds to the droplet formation time. In order to gain some insights in the time scales involved on the molecular mixing of the two fluids within the droplets, we calculated the temporal evolution of the concentration profiles involved in the Fick interdiffusion of the two streams of interest in a coflow scenario.[13,14,26] The corresponding concentration profiles are represented with plain lines on Fig. 6a. This simple model assumes only a one-dimensional diffusion along the x direction, but has the virtue of comparing the molecular mixing measured within the flowing droplets to the pure diffusive mixing configuration of a coflow. In the present model, the initial $K_4Fe(CN)_6$ and $K_3Fe(CN)_6$ concentration profiles are characterized by a "step"-like distribution given by the following expressions:

$$C\left(K_4Fe(CN)_6\right)\begin{cases} C = C_0 & \text{for} \quad 0 \le x \le {}^{w_{chn}}/_2 \\ C = 0 & \text{for} \quad {}^{w_{chn}}/_2 \le x \le w_{chn} \end{cases}$$

$$C\left(K_3Fe(CN)_6\right)\begin{cases} C = 0 & \text{for} \quad 0 \le x \le {}^{w_{chn}}/_2 \\ C = C_0 & \text{for} \quad {}^{w_{chn}}/_2 \le x \le w_{chn} \end{cases}$$

The temporal evolution of such concentrations $C(x,t)$ is well known and follows for dilute solutions the diffusion law[26] given by:

$$\frac{C(x,t)}{C_0} = \frac{1}{2}\sum_{n=-\infty}^{n=+\infty}\left[\operatorname{erf}\left(\frac{{}^{w_{chn}}/_2 + 2n\,w_{chn} - x}{2\sqrt{Dt}}\right) + \operatorname{erf}\left(\frac{{}^{w_{chn}}/_2 - 2n\,w_{chn} + x}{2\sqrt{Dt}}\right)\right]$$

where D stands for the diffusion coefficient of the solute molecule of interest ($D = 0.89 \times 10^{-5}$ cm^2 s^{-1} for $K_3Fe(CN)_6$ and 0.74×10^{-5} cm^2 s^{-1} for $K_4Fe(CN)_6$) and erf represents the error function given by:

$$\operatorname{erf}(z) = \int_0^z \exp\left(-\eta^2\right)\,d\eta$$

By analyzing both sets of data in Fig. 6a, it is possible to emphasize the effect of the droplet forced internal advection in the mixing.[27] In fact, when droplets are squished by the upper walls of the channels, a forced advection regime is created inside them.[28] Within the reference frame of the droplets, periodic fluid recirculation loops spontaneously form and exhibit an axial symmetry parallel to the droplet translation direction.[29] It is has been proved that when unmixed droplets encounter angle bends in their trajectory, the shear rate induced by the bends dramatically enhances mixing.[5,6,28] In this work, we detach from quantifying the

 This journal is © The Royal Society of Chemistry 2006

View Article Online

Published on 06 June 2006. Downloaded on 25/01/2016 00:28:05.

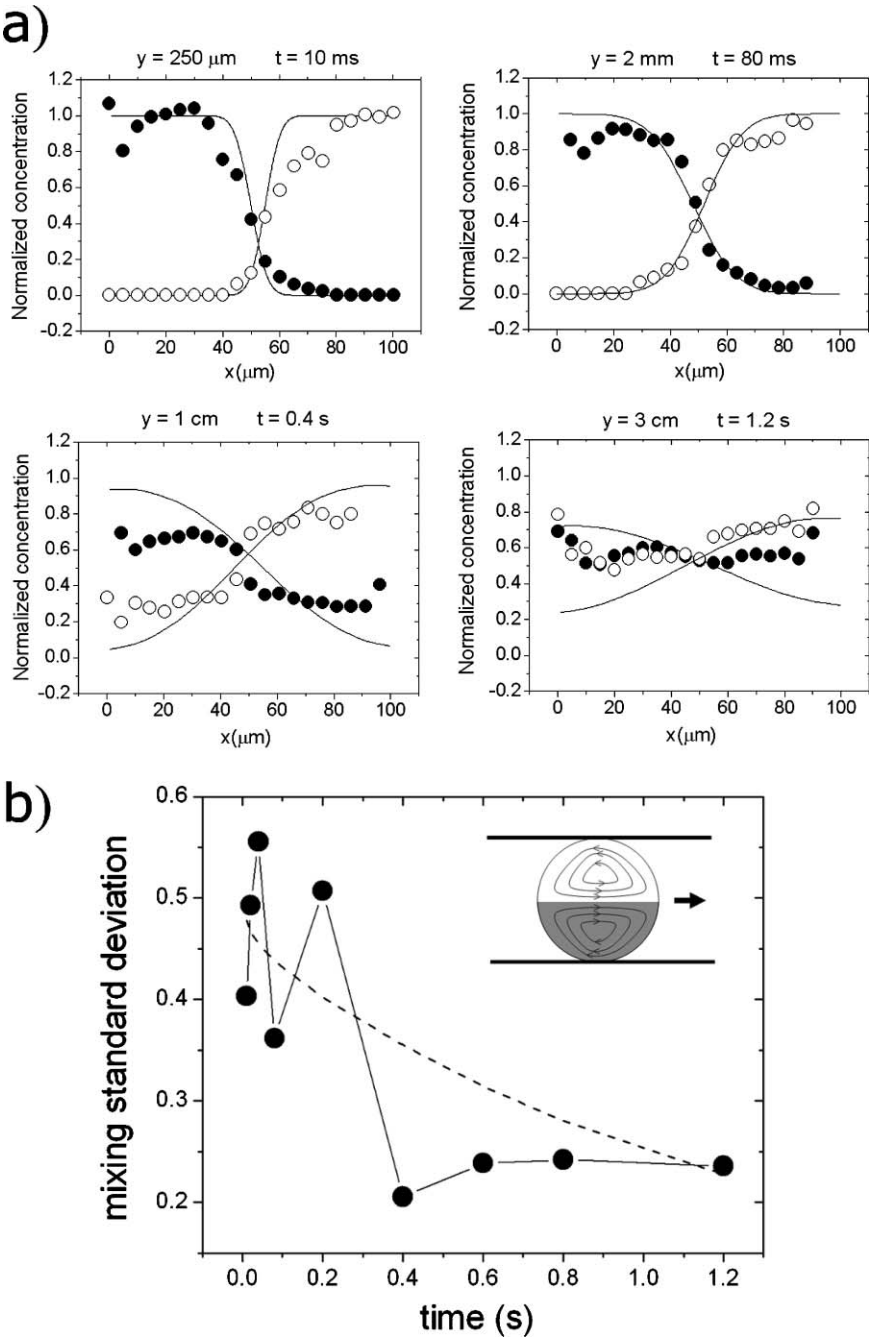

Fig. 6 (a) Corrected droplet concentration profiles as a function of x at different y positions. Black and open dots respectively represent the measured profiles of the $K_4Fe(CN)_6$ and the $K_3Fe(CN)_6$ solutions. The lines drown in the figures represent the theoretical concentration profiles obtained in a coflow configuration. (b) Evolution of the mixing standard deviation within the droplets (dark circles) and in the theoretical diffusion driven mixing scenario (dashed line). Inset: schematics of the droplet internal streamlines in the reference frame of the droplet when it flows in a channel.

best mixing scenarios but we analyze the effect of the coupling between the molecular diffusion and the forced advection on the droplet internal mixing in a straight channel devoid of angle bends.

Interestingly, at the very early stages (typically before 200 ms), the two aqueous solutions remain localized in their original droplet hemisphere. Nor "cross-contamination" neither significant interdiffusion is observed. The inner droplet concentration profiles match almost perfectly the expected profiles obtained for the case of the pure diffusive scenario. We have established a mixing criterion in order to compare for each compound the two sets of data. By calculating the standard deviation of the normalized concentration profiles respect their mean value (Fig. 6b), it is possible to distinguish a poorly mixed situation with respect a well mixed situation. An unmixed scenario which is characterised by a "step"-like normalized concentration profile presents a standard deviation close to 0.5 and converges towards zero as the mixing becomes more and more efficient. We report in Fig. 6b the evolution for

View Article Online

Published on 06 June 2006. Downloaded on 25/01/2016 00:28:05.

the $K_4Fe(CN)_6$ solution of the mixing standard deviation in the droplet and the coflow case at different lifetimes.

At the initial lifetimes, the droplet and the coflow approximation present comparable values of the standard deviation. In the early stages, mixing is dominated by diffusion and the forced internal advection has no effect. Once the solutions start to interdiffuse more importantly, the overall mixing is accelerated and a sudden change is observed around 300 ms. The droplet hydrodynamics characterized by the forced advection become dominant over diffusion as it is seen in Fig. 6b. The molecules having diffused to the "opposite" hemisphere are redistributed by the droplet internal streamlines in the whole opposite hemisphere. This results on a sudden take-off of the concentration profiles at the opposite regions of the droplets (Fig. 6a). The subsequent effect is to dramatically lower the mixing criterion as complete mixing is almost achieved. Afterwards, whereas in the pure diffusive approximation the mixing standard deviation continues to slowly evolve until reaching its final value of zero, in the droplet case no further evolution is measured. It clearly appears that the coupling between diffusion and the droplet internal forced advection accelerates mixing respect the diffusive coflow case. This acceleration strongly depends on different factors as the droplet size, droplet velocity, channel form factor, fluid viscosities and the diffusion coefficient of the solutes among others. In the present study complete mixing time within the droplet has been improved by a factor of three respects the pure diffusive scenario and has been determined to be around 400 ms.

IV. Conclusion

In this paper we have shown that it is possible to probe *in situ* the composition of droplets circulating in microchannels by using Raman spectroscopy. Such droplets appear as almost ideal chemical reactors, as they can host very rapid and exothermical chemical reactions and can drive them in controlled conditions. We have demonstrated that confocal Raman microspectroscopy is an approach that is very well adapted to probing the chemical composition of such droplets, which strongly indicates the value of developing this approach for the investigation of chemical reactions. We have shown that the measurements were specific, quantitative and local and we have suggested an approach to extract the concentration profiles of chemical species within travelling droplets for a wide range of droplet sizes and droplet production frequencies. We have been able to monitor the evolution of mixing within "Janus" droplets. In such circulating droplets, the initial steps of mixing are first dominated by diffusion and then progressively by advection. Finally, this work paves the way for future studies involving systematic investigations of complex chemical reactions by Raman spectroscopy in droplets, and by using statistical methods (chemometrics) for the analysis of the chemical data. Additionally, this experimental approach may support and complement various theoretical and numerical investigations concerning droplet generation, droplet break-up and complex internal flow circulations.[30]

Acknowledgements

This work was supported by CNRS Programme Interdisciplinaire de Recherche "Microfluidique et Systèmes Fluidiques". The authors acknowledge the Université Bordeaux I, the Conseil Régional d'Aquitaine and FEDER funds for their financial support. Jean-Baptiste Salmon and Bertrand Pavageau are gratefully acknowledged for fruitful discussions.

References

1 T. M. Squires and S. R. Quake, *Rev. Mod. Phys.*, 2005, **77**, 977–1026.
2 H. A. Stone, A. D. Stroock and A. Ajdari, *Ann. Rev. Fluid Mech.*, 2004, **36**, 381–411.
3 M. A. Burns, B. N. Johnson, S. N. Brahmasandra, K. Handique, J. R. Webster, M. Krishnan, T. S. Sammarco, P. M. Man, D. Jones, D. Heldsinger, C. H. Mastrangelo and D. T. Burke, *Science*, 1998, **282**, 484–487.
4 M. A. Burns, *Science*, 2002, **296**, 1818–1819.
5 H. Song, J. D. Tice and R. F. Ismagilov, *Angew. Chem., Int. Ed.*, 2003, **42**, 767–772.
6 M. R. Bringer, C. J. Gerdts, H. Song, J. D. Tice and R. F. Ismagilov, *Philos. Trans. R. Soc. London, Ser. A*, 2004, **362**, 1087–1104.
7 M. Joanicot and A. Ajdari, *Science*, 2005, **309**, 887–888.
8 S. L. Anna, N. Bontoux and H. A. Stone, *Appl. Phys. Lett.*, 2003, **82**, 3, 264–366.
9 P. Guillot and A. Colin, *Phys. Rev. E*, 2005, **72**, 1.
10 C. Amatore, F. Bonhomme, J. L. Bruneel, L. Servant and L. Thouin, *J. Electroanal. Chem.*, 2000, **1**, 1–17.
11 I. Rey, J. L. Bruneel, J. Girondin, L. Servant and J. C. Lassegues, *J. Electromech. Soc.*, 1998, **145**, 3034–3042.
12 P. Hinsmann, J. Frank, M. Harasek and B. Lendl, *Lab Chip*, 2001, **1**, 16.
13 J. B. Salmon, A. Ajdari, P. Tabeling, L. Servant, D. Talaga and M. Joanicot, *Appl. Phys. Lett.*, 2005, **86**, 094106.
14 A. E. Kamholz, B. H. Weigl, B. A. Finlayson and P. Yager, *Anal. Chem.*, 1999, **71**, 5340–5347.
15 D. Qin, Y. Xia and G. M. Whitesides, *Adv. Mater.*, 1996, **8**, 917–921.
16 D. C. Duffy, J. C. McDonald, O. J. A. Schueller and G. M. Whitesides, *Anal. Chem.*, 1998, **70**, 4974–4984.
17 J. C. McDonald, D. C. Duffy, J. R. Anderson, D. T. Chiu, H. Wu, O. J. A. Schueller and G. M. Whitesides, *Electrophoresis*, 2000, **21**, 27–40.
18 Y. Xia and G. M. Whitesides, *Angew. Chem., Int. Ed.*, 1998, **37**, 550–575.
19 C. Harrison, J. T. Cabral, C. M. Stafford, A. Karim and E. J. Amis, *J. Micromech. Microeng.*, 2004, **14**, 153–158.
20 T. Thorsen, F. H. Roberts, F. H. Arnold and S. R. Quake, *Phys. Rev. Lett.*, 2001, **86**, 4163.
21 D. R. Link, S. L. Anna, D. A. Weitz and H. A. Stone, *Phys.Rev.Lett.*, 2004, **92**, 054503.
22 R. Dreyfus, P. Tabeling, and H. Willaime, *Phys. Rev. Lett.*, 2003, **90**, 144505.
23 Y. Tan, J. S. Fisher, A. I. Lee, V. Cristtini and A. P. Lee, *Lab Chip*, 2004, **4**, 292–298.
24 P. Garstecki, H. A. Stone and G. M. Whitesides, *Phys. Rev. Lett.*, 2005, **94**, 164501.
25 J. M. Gordillo, Z. Cheng, A. M. Ganan-Calvo, M. Marquez and D. A. Weitz, *Phys. Fluids*, 2004, **16**, 2828–2834.
26 J. Crank. *Mathematics of Diffusion*, Clarendon, Oxford, 2nd edn, 1975.
27 Z. B. Stone and H. A. Stone, *Phys. Fluids*, 2005, **17**, 063103.
28 F. Sarrazin, L. Prat, N. Di Miceli, G. Cristobal, D. R. Link, and D. A. Weitz, *Chem. Eng. Sci.*, submitted.
29 C. Coulliette and C. Pozrikidis, *J.Fluid Mech.*, 1998, **358**, 1–28.
30 V. Cristini and Y. C. Tan, *Lab Chip*, 2004, **4**, 257.

 This journal is © The Royal Society of Chemistry 2006